J. Fluid Mech. (1980), *vol.* 97, *part.* 4, *pp.* 721–742
Printed in Great Britain

The attenuation of water waves over a non-rigid bed

By HUGH MACPHERSON

Department of Theoretical and Applied Mechanics,
School of Mathematics, University of New South Wales, Australia

(Received 24 October 1978 and in revised form 24 April 1979)

Water waves that propagate over a non-rigid bed are attenuated as a result of energy dissipation within the bed. This paper describes the analysis, from the basis of small-amplitude wave theory, of the coupled interaction between the bed, which responds in both an elastic and viscous manner, and an overlying layer of inviscid fluid. A dispersion relation is derived, from which rates of wave attenuation and sea bed deflexions are calculated.

The results are relevant wherever the sea bed, in its response to water waves, is non-rigid, as is often the case in coastal waters. Depending on the elasticity and viscosity of the sea bed, the wave attenuation can be of the same or of a larger order of magnitude than that due to bottom friction or percolation in a permeable bed. Where waves propagate over a soft viscous bed, for example as is the case at certain mud flats off the south-west coast of India, exceptionally high rates of attenuation are possible whereby waves are almost completely damped within several wavelengths.

1. Introduction

When waves are attenuated in coastal waters, the mechanism of energy dissipation generally involves some form of bottom interaction. Most theories of wave attenuation, such as that owing to bottom friction or to percolation in a permeable bed, are based on the assumption that the bed is rigid in its response to water waves. There is increasing evidence, however, that, as waves propagate over the sea bed, small deflexions can be induced in the sea bed itself. Bjerrum (1973) writes of North Sea waves causing sea-bed deflexions of up to 5 cm. Associated with such deflexions, there is inevitably some dissipation of wave energy due to internal friction within the sea bed. This mechanism may be a contributing factor in an explanation of wave attenuation over continental shelves and in coastal waters. Hasselmann *et al.* (1973) have made measurements of swell propagation and attenuation in the North Sea. They attempted to correlate observed rates of swell attenuation with the theory of attenuation due to bottom friction. However, a significant prediction of this theory, namely that there should be a strong modification of the swell decay rates by tidal currents, was not observed in the extensive swell data. It appears, therefore, that some other mechanism (or mechanisms) is involved. It is possible that the sea bed is not rigid and that the wave attenuation is caused by energy dissipation within the sea bed.

Where the bed responds in both an elastic and viscous manner, the elastic response is in the form of a restoring force, i.e. restoring the bed to its undisturbed position, while the viscous response is in the form of a dissipative force (internal friction) which is the cause of the wave attenuation. The first theoretical investigation of this problem

0022–1120/80/4430–8610 $02.00

was undertaken by Gade (1959) who studied the coupled interaction between a shallow layer of an inviscid fluid overlying an incompressible non-rigid bed of infinite depth. He derived a dispersion relation in the form of several simultaneous equations which he solved to yield the wave attenuation and the relative magnitude of the sea-bed displacement. In the present study the problem is analysed from the basis of small-amplitude wave theory such that a wider range of results are obtained for any depth of either the lower or upper layer.

In § 2 we discuss the Voigt model for the sea-bed material; this model conveniently combines the viscosity and elasticity of the bed. The linearized governing equations, which for the bed are almost identical to the linearized Navier–Stokes equations, and the boundary conditions are derived. In § 3 we determine the dispersion relation for damped travelling waves. An explicit expression is derived for the wave attenuation and sea-bed displacement when this displacement is small relative to the surface wave amplitude. In § 4 the dispersion relation is solved to yield exact numerical results for wave attenuation and for the relationships between the surface and interface profiles. The energy dissipation rates of the present theory are compared with dissipation rates due to other mechanisms such as those due to bottom friction or percolation in a permeable bed.

In § 5 we explore the physical relevance of this study firstly to waves propagating over an almost rigid bed, as is often the case in coastal waters, and secondly to waves propagating over a soft viscous bed. In the latter case, where the bed elasticity is negligible, we obtain results similar to those of Gade (1958) and Dalrymple & Liu (1978). From these results it is shown that waves can be almost completely attenuated over a distance of several wavelengths. Such dramatic rates of wave attenuation have been observed at certain coastal localities, such as off the south-west coast of India, where the sea bed is a soft viscous mud (MacPherson & Kurup 1979).

2. Formulation

2.1. *The viscoelastic model*

In a non-rigid medium within which there is both an elastic and a viscous response to a small disturbance, we can refer to the medium as viscoelastic. One of the simplest ways to combine the viscosity and elasticity in the medium is to use the Voigt model. The mechanical representation of this is a spring and dashpot in parallel so that, on loading, the deflexion of the system asymptotically approaches a constant value and when the load is removed the system steadily recovers. The spring is taken to obey Hooke's law and the dashpot can be considered as a piston being drawn through a Newtonian fluid. In this paper we will use the Voigt model because, as shown below, the governing equations for the viscoelastic medium are almost identical to the governing equations for a viscous fluid.

The linearized equations of motion for a small disturbance of an incompressible, viscoelastic medium are (Kolsky 1963)

$$\frac{\partial^2 \mathbf{x}}{\partial t^2} = -\frac{1}{\rho}\nabla p + \nu \frac{\partial}{\partial t}\nabla^2 \mathbf{x} + \frac{G}{\rho}\nabla^2 \mathbf{x} - \mathbf{g}, \tag{2.1}$$

where $\mathbf{x}$ are particle displacements, ν is the kinematic viscosity, G the shear modulus of elasticity and $\mathbf{g}$ the vertical acceleration due to gravity. We can replace $\partial^2 \mathbf{x}/\partial t^2$

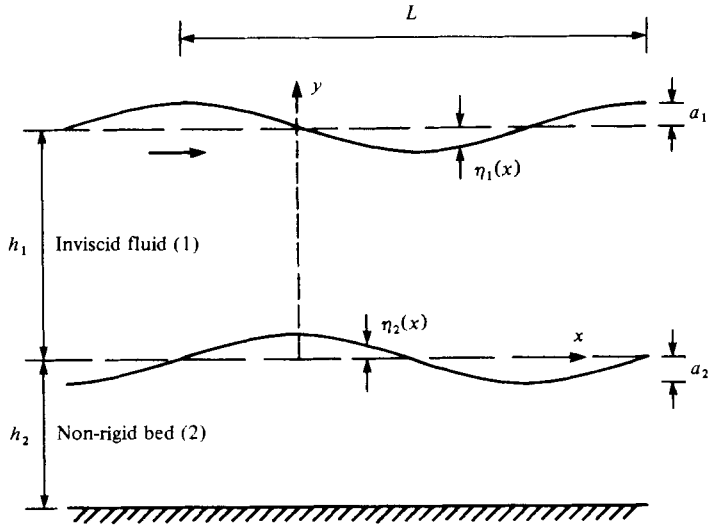

FIGURE 1. Definition sketch.

by the velocities $\partial\mathbf{u}/\partial t$ and, if we assume that the disturbance varies sinusoidally in time such that $\mathbf{x}$ and $\mathbf{u}$ vary as $\exp(-i\sigma t)$, we can replace $\partial(\nabla^2\mathbf{x})/\partial t$ by $\nabla^2\mathbf{u}$ and $\nabla^2\mathbf{x}$ by $\nabla^2\mathbf{u}/(-i\sigma)$ to obtain

$$\frac{\partial\mathbf{u}}{\partial t} = -\frac{1}{\rho}\nabla p + \left(\nu + \frac{iG}{\rho\sigma}\right)\nabla^2\mathbf{u} - \mathbf{g}. \tag{2.2}$$

We can now introduce a viscoelastic parameter, ν_e, where

$$\nu_e = \nu + iG/\sigma\rho, \tag{2.3}$$

such that ν_e is complex, the real part being the viscosity and the imaginary part being a measure of the elasticity. Thus the equations of motion for a viscoelastic medium have reduced to the form of the linearized Navier–Stokes equations for a viscous fluid. As was shown by Tchen (1956), by using the Voigt model the study of waves in a viscoelastic medium parallels the study of waves in a viscous fluid.

2.2. *The governing equations*

We first present the linearized governing equations for small-amplitude water waves propagating over a viscoelastic bed of finite depth. We take the linearized form of these equations because, having made the assumption that the waves are of small amplitude, the velocities are small and their products can be neglected. In two dimensions, Cartesian co-ordinates (x, y) are introduced such that the origin is at the undisturbed interface between the two layers and y is positive upwards as shown in figure 1. Subscripts 1 and 2 refer to the upper and lower layers respectively. The elevation of the upper surface of the water is defined by $y = h_1 + \eta_1$, where h_1 is the mean depth. The elevation of the interface, which is common to both layers, is defined by $y = \eta_2$. It is assumed that there is no mixing at the interface and that the density of the lower layer, ρ_2, is greater than the density of the upper layer, ρ_1.

For the *lower* layer, the bed is modelled as an incompressible viscoelastic medium and, from equation (2.2), the equations of motion are

$$\frac{\partial u_2}{\partial t} = -\frac{1}{\rho_2}\frac{\partial p_2}{\partial x} + \nu_e \nabla^2 u_2, \tag{2.4a}$$

$$\frac{\partial v_2}{\partial t} = -\frac{1}{\rho_2}\frac{\partial p_2}{\partial y} + \nu_e \nabla^2 v_2 - g, \tag{2.4b}$$

where we tacitly drop the subscript 2 for the viscoelastic parameter ν_e, and the continuity equation is

$$\frac{\partial u_2}{\partial x} + \frac{\partial v_2}{\partial y} = 0. \tag{2.5}$$

Because the linearized Navier–Stokes equations allow for the velocities u_2 and v_2 to be split into a potential part and a rotational part, we introduce (here we follow Lamb 1932) a velocity potential ϕ_2 and a stream function ψ_2 such that

$$u_2 = -\frac{\partial \phi_2}{\partial x} - \frac{\partial \psi_2}{\partial y}, \quad v_2 = -\frac{\partial \phi_2}{\partial y} + \frac{\partial \psi_2}{\partial x}, \tag{2.6}$$

$$\nabla^2 \phi_2 = 0, \tag{2.7}$$

and

$$\nu_e \nabla^2 \psi_2 = \frac{\partial \psi_2}{\partial t}. \tag{2.8}$$

The pressure, p_2, is determined solely from the potential part by the relationship

$$p_2 = \rho_2 \frac{\partial \phi_2}{\partial t} - \rho_2 g y. \tag{2.9}$$

For the *upper* layer, the water is assumed to have negligible viscosity. We can, therefore, take the flow to be irrotational and can introduce a velocity potential ϕ_1 such that

$$u_1 = -\frac{\partial \phi_1}{\partial x}, \quad v_1 = -\frac{\partial \phi_1}{\partial y}. \tag{2.10}$$

The pressure, p_1, is evaluated from

$$p_1 = \rho_1 \frac{\partial \phi_1}{\partial t} - \rho_1 g y, \tag{2.11}$$

and the governing equation for the motion in the upper layer is

$$\nabla^2 \phi_1 = 0. \tag{2.12}$$

In seeking a solution to the governing equations (2.7), (2.8) and (2.12) we must satisfy the appropriate boundary conditions.

2.3. *Boundary conditions*

The linearized boundary conditions can be enumerated as follows:

(1) At the interface between the water and the non-rigid bed there must be continuity of shear stress. Since we assume that no shear stress can be sustained by the water, then we must take the shear stress in the lower layer at the interface to be zero. This can be written

$$\rho_2 \nu_e (u_{2y} + v_{2x}) = 0 \quad \text{on} \quad y = 0. \tag{2.13}$$

Using equation (2.6), the shear stress condition becomes

$$-2\phi_{2xy}-\psi_{2yy}+\psi_{2xx}=0 \quad \text{on} \quad y=0. \tag{2.14}$$

(2) The kinematic condition at the interface is the requirement that there is continuity of normal velocity. In its linearized form, however, this condition requires only continuity of vertical velocity, i.e. such that the two layers always stay in contact, but allows for a discontinuity in the horizontal velocity. This discontinuity is acceptable because we have assumed that the water is acting as a perfect fluid. With η_2 representing the profile at the interface then the linearized kinematic condition is

$$\eta_{2t}=v_2=v_1 \quad \text{on} \quad y=0. \tag{2.15}$$

In terms of the velocity potential and stream function we have

$$\eta_{2t}=-\phi_{2y}+\psi_{2x}=-\phi_{1y} \quad \text{on} \quad y=0. \tag{2.16}$$

(3) At the upper surface of the water we have the linearized kinematic condition that

$$\eta_{1t}=v_1=-\phi_{1y} \quad \text{on} \quad y=h_1. \tag{2.17}$$

We assume that the dynamic variations in pressure above the upper surface are negligible and therefore we take the pressure, p_1, as given by equation (2.11), to be constant at $y=h_1+\eta_1$. This pressure condition and the kinematic condition given by (2.17) can be combined to give the conventional free-surface boundary condition for irrotational water waves:

$$\phi_{1tt}+g\phi_{1y}=0 \quad \text{on} \quad y=h_1. \tag{2.18}$$

(4) The dynamic condition at the interface requires that the normal stresses must be balanced by the surface tension T. Thus, we can write the boundary condition

$$\left(-p_2+2\rho_2\nu_e\frac{\partial v_2}{\partial y}\right)_{y=\eta_2}-(-p_1)_{y=\eta_2}=T\frac{\partial^2\eta_2}{\partial x^2}. \tag{2.19}$$

Using equations (2.11) and (2.9) to obtain p_1 and p_2 at $y=\eta_2$ respectively, the dynamic condition can be rewritten in its linearized form

$$-\rho_2\phi_{2t}+\rho_2 g\eta_2+2\rho_2\nu_e v_{2y}+\rho_1\phi_{1t}-\rho_1 g\eta_2=T\eta_{2xx} \quad \text{on} \quad y=0. \tag{2.20}$$

(5) And the final condition, for a bed of finite depth at $y=-h_2$, is that we require the horizontal and vertical velocities to be zero at the rigid horizontal bed. In terms of the velocity potential and stream function for the lower layer the two boundary conditions can be written

$$u_2=-\phi_{2x}-\psi_{2y}=0 \quad \text{on} \quad y=-h_2, \tag{2.21}$$

$$v_2=-\phi_{2y}+\psi_{2x}=0 \quad \text{on} \quad y=-h_2. \tag{2.22}$$

If the sea bed is of infinite depth, then we would require that both ϕ_2 and ψ_2 vanish as $y\to-\infty$.

3. Solution for damped travelling waves

3.1. *Derivation of the dispersion relation*

We shall consider a profile at the interface between the water and the bed to be of the form

$$\eta_2 = a_2 \exp[i(mx - \sigma t)], \tag{3.1}$$

where it is understood that we take only the real part of the right-hand side. For progressive waves that decay with distance we take the radian frequency σ as real and the complex wavenumber as

$$m = k + iD, \tag{3.2}$$

so the real part of equation (3.1) can be written

$$\eta_2 = a_2 e^{-Dx} \cos(kx - \sigma t), \tag{3.3}$$

which is a progressive wave of amplitude $a_2 \exp(-Dx)$, where a_2 is real and D is the decay parameter. The wavenumber k and radian frequency σ are common to both layers.

We seek a solution to the governing equations and boundary conditions by choosing ϕ_2, ψ_2 and ϕ_1 of the form

$$\phi_2 = \frac{i}{m}[Al \cosh m(y + h_2) + Cm \sinh m(y + h_2)] \exp[i(mx - \sigma t)], \tag{3.4}$$

$$\psi_2 = [C \cosh l(y + h_2) + A \sinh l(y + h_2)] \exp[i(mx - \sigma t)], \tag{3.5}$$

$$\phi_1 = (E \cosh my + F \sinh my) \exp[i(mx - \sigma t)], \tag{3.6}$$

where again we only take the real part of the right-hand side of these equations. Equations (3.4) and (3.5) already satisfy the boundary conditions at the rigid bed on $y = -h_2$. Equations (2.7), (2.8) and (2.12) are satisfied when

$$l = (m^2 - i\sigma/\nu_e)^{\frac{1}{2}}, \tag{3.7}$$

where without loss of generality we take l to be defined such that its real part is positive.

The relationship between C and A is found by substituting (3.4) and (3.5) into the shear-stress boundary condition (2.14):

$$\frac{C}{A} = \frac{2ml \sinh mh_2 - (m^2 + l^2) \sinh lh_2}{2m^2 \cosh mh_2 - (m^2 + l^2) \cosh lh_2}. \tag{3.8}$$

From equations (3.4) and (3.5) and the kinematic boundary condition (2.16) we obtain an expression for the interface profile of the form

$$\eta_2 = \frac{B}{2im\nu_e} \exp[i(mx - \sigma t)], \tag{3.9}$$

where

$$B = C \cosh lh_2 + A \sinh lh_2. \tag{3.10}$$

From (3.9) and (3.1) we find that

$$a_2 = B/2im\nu_e, \tag{3.11}$$

which, we recall, is real. The relationship between F and B, from equations (3.4), (3.5) and (3.6) and the boundary condition (2.16), is

$$\frac{F}{B} = \frac{\sigma}{2m^2\nu_e}, \tag{3.12}$$

and the relationship between E and F is, from equation (3.6) and the free surface boundary condition (2.18),

$$\frac{E}{F} = -\frac{gm\cosh mh_1 - \sigma^2 \sinh mh_1}{gm\sinh mh_1 - \sigma^2\cosh mh_1}. \tag{3.13}$$

Thus we can now rewrite the velocity potential in the upper fluid, by substituting equations (3.12) and (3.13) into (3.6), in the form

$$\phi_1 = -\frac{B\sigma}{2m^2\nu_e}\left[\frac{gm\cosh(mh_1 - my) - \sigma^2\sinh(mh_1 - my)}{gm\sinh mh_1 - \sigma^2\cosh mh_1}\right]\exp[i(mx-\sigma t)]. \tag{3.14}$$

From equations (2.17) and (3.14) we find that the upper surface profile at $y = h_1 + \eta_1$ can be expressed in the form

$$\eta_1 = \frac{B}{2im^2\nu_e}\left[\frac{\sigma^2}{\sigma^2\cosh mh_1 - gm\sinh mh_1}\right]\exp[i(mx-\sigma t)]. \tag{3.15}$$

The ratio of the interface profile, η_2, to the upper surface profile, η_1, from (3.9) and (3.15), is

$$\eta_2/\eta_1 = \cosh mh_1 - (gm/\sigma^2)\sinh mh_1, \tag{3.16}$$

which corresponds to the ratio given by Lamb (1932) for two inviscid layers of different density. From equation (3.16) the amplitude ratio is

$$a_2/a_1 = |\cosh mh_1 - (gm/\sigma^2)\sinh mh_1|, \tag{3.17}$$

and the phase angle, θ, between the surface profile and the interface profile is

$$\theta = -\arg\{\cosh mh_1 - (gm/\sigma^2)\sinh mh_1\} \tag{3.18}$$

such that a positive value of θ indicates that the surface profile lags behind the interface profile. The free-surface profile can now be expressed in the form

$$\eta_1 = a_1 e^{-Dx}\cos(kx - \sigma t + \theta), \tag{3.19}$$

where $a_1\exp(-Dx)$ is the modulus of equation (3.15).

Finally, substituting the necessary equations into the dynamic boundary condition (2.20), we obtain an expression relating σ and m which can be rearranged to yield

$$\begin{aligned}&\frac{\rho_1(\sigma^4 - g^2m^2)\tanh mh_1}{gm\tanh mh_1 - \sigma^2} + \rho_2 gm + Tm^3\\ &+\rho_2(2m^2\nu_e - i\sigma)^2\left\{\frac{(2m^2 - i\sigma/\nu_e)[lC_mC_l - mS_mS_l] - 2m^2l}{(2m^2 - i\sigma/\nu_e)[lS_mC_l - mC_mS_l]}\right\}\\ &-4\rho_2 m^3\nu_e^2 l\left\{\frac{(2m^2 - i\sigma/\nu_e) - 2m[mC_mC_l - lS_mS_l]}{2m[lS_mC_l - mC_mS_l]}\right\} = 0,\end{aligned} \tag{3.20}$$

where

$$\left.\begin{aligned}C_m &= \cosh mh_2, \quad C_l = \cosh lh_2,\\ S_m &= \sinh mh_2, \quad S_l = \sinh lh_2.\end{aligned}\right\} \tag{3.21}$$

This is the dispersion relation from which it is possible to determine m, i.e. the wave-number k and the rate of decay D, in terms of all physical parameters of the problem: σ, h_1, h_2, ρ_1, ρ_2, T and ν_2.

In the limiting case when the upper fluid is absent, i.e. for a single layer of viscous fluid, we put h_1 or ρ_1 to zero, replace ν_e by ν and we recover the dispersion relation given by Wehausen & Laitone [1960, equation (25.36)]. Alternatively in the limiting case of two inviscid, inelastic layers, we let $\nu_e \to 0$ in (3.20) and obtain the classical two-layer dispersion relation (Lamb 1932, p. 372).

For the case of long waves, i.e. when the combined water and non-rigid bed depth is small in comparison to the wavelength, and when the parameter $(m^2\nu_e/\sigma)$ is small, it can be shown that equation (3.20) reduces to the biquadratic in m:

$$m^4 g^2 \gamma h_1 h_2 \Gamma - m^2 \sigma^2 g(h_1 + h_2\Gamma) + \sigma^4 = 0, \tag{3.22}$$

with

$$\gamma = 1 - \rho_2/\rho_1 \tag{3.23}$$

and

$$\Gamma = 1 - \frac{\tanh(-ih_2^2\sigma/\nu_e)^{\frac{1}{2}}}{(-ih_2^2\sigma/\nu_e)^{\frac{1}{2}}}, \tag{3.24}$$

where we have tacitly dropped the surface tension T. For the case of a purely viscous bed, i.e. $\nu_e \to \nu$, then (3.22) and (3.24) reduce to the results given by Gade (1958). For the case of a purely elastic bed, $\nu_e \to iG/\rho_2\sigma$, and thus (3.24) becomes

$$\Gamma_{\nu=0} = 1 - \frac{\tan(\rho_2 h_2^2 \sigma^2/G)^{\frac{1}{2}}}{(\rho_2 h_2^2 \sigma^2/G)^{\frac{1}{2}}} \tag{3.25}$$

for which it can be shown that there is zero decay. Mallard & Dalrymple (1977) show that when waves propagate over a purely elastic bed as expected there is zero decay.

For the case when the lower layer is of infinite depth we let $h_2 \to \infty$ in (3.20) and, after some rearranging, we get

$$\frac{\frac{\rho_1}{\rho_2}\left[1 - \left(\frac{gm}{\sigma^2}\right)^2\right]\tanh mh_1}{\left(\frac{gm}{\sigma^2}\right)\tanh mh_1 - 1} + \frac{gm}{\sigma^2} - \left(1 + \frac{2im^2\nu_e}{\sigma}\right)^2 + \left(\frac{2im^2\nu_e}{\sigma}\right)^2 \left(1 + \frac{\sigma}{im^2\nu_e}\right)^{\frac{1}{2}} = 0. \tag{3.26}$$

We can check the validity of this result for two cases when the upper fluid is absent; firstly for waves in a semi-infinite viscous medium we recover the result given by Wehausen & Laitone [1960, equation (25.17)], and secondly for waves in a semi-infinite elastic medium we recover the result given by Bromwich (1898).

3.2. *Explicit solution for an almost rigid bed*

Apart from unusual localities where the sea bed is a soft viscous mud, the oscillations of the sea bed due to the propagating waves will be, at most, small in comparison to the surface waves. In such cases of a small response, we refer to the sea bed as 'almost rigid'. The resistance of the bed to movement is in general due to relatively high values of either the bed viscosity or the bed elasticity. To obtain an explicit expression for the decay of waves over an almost rigid bed, we make an assumption about the

non-dimensional parameter $(m^2\nu_e/\sigma)$. This parameter, as it occurs in the dispersion relation, can be written

$$im^2\nu_e/\sigma = im^2\nu/\sigma - m^2G/\sigma^2\rho_2. \tag{3.27}$$

The first parameter on the right is a non-dimensional measure of the viscous response; the second is a non-dimensional measure of the elastic response.

For an almost rigid bed where either the values of viscosity are high, $m^2\nu/\sigma \gg 1$, or the values of elasticity are high, $m^2G/\rho_2\sigma^2 \gg 1$, we can take the absolute magnitude of $m^2\nu_e/\sigma$ to be large, i.e. $|m^2\nu_e/\sigma| \gg 1$. Taking the dispersion relation, equation (3.26), for the case when the lower layer is of infinite depth, we expand the square-root term in a series and rearrange, rejecting terms of order $\sigma/m^2\nu_e$, to obtain

$$\frac{\dfrac{\rho_1}{\rho_2}\left[1-\left(\dfrac{gm}{\sigma^2}\right)^2\right]\tanh mh_1}{\left(\dfrac{gm}{\sigma^2}\right)\tanh mh_1 - 1} + \frac{gm}{\sigma^2} - \frac{2im^2\nu_e}{\sigma} - \frac{3}{2} = O\left(\frac{\sigma}{m^2\nu_e}\right). \tag{3.28}$$

As a further assumption we take the wavelength to be long compared to the water depth, as is often the case in coastal waters, and express $\tanh mh_1$ in series form. We now non-dimensionalize by defining $m^* = m(gh_1)^{\frac{1}{2}}/\sigma$, $\sigma^* = \sigma(h_1/g)^{\frac{1}{2}}$, $\rho^* = \rho_1/\rho_2$ and $\nu_e^* = (\nu + iG/\rho_2\sigma)(gh_1^3)^{-\frac{1}{2}}$. Because ν_e^* is complex, it is the modulus of ν_e^* that we now take to be large. By expanding m^* in (3.28) in powers of $(\nu_e^*)^{-1}$,

$$m^* = 1 + m_1^*(\nu_e^*)^{-1} + m_2^*(\nu_e^*)^{-2} + \ldots \tag{3.29}$$

and equating terms we find, after some work, that

$$m^* \approx 1 + \frac{i\rho^*}{4\sigma^*\nu_e^*} \tag{3.30}$$

to the first order in ν_e^{*-1}. In dimensional terms, and on replacing ν_e by $(\nu + iG/\rho_2\sigma)$, we obtain

$$m \approx \frac{\sigma}{(gh_1)^{\frac{1}{2}}} + \frac{\rho_1 gG}{4\rho_2^2\sigma^2(\nu^2 + G^2/\rho_2^2\sigma^2)} + \frac{i\rho_1 g\nu}{4\rho_2\sigma(\nu^2 + G^2/\rho_2^2\sigma^2)}. \tag{3.31}$$

Now $m = k + iD$, so by equating the real parts we find that the wavenumber is given by the first two terms on the right, the second being only a small modification to the first, $\sigma/(gh_1)^{\frac{1}{2}}$, which is the long-wave rigid-bed wavenumber. By equating the imaginary parts, the rate of decay is

$$D \approx \frac{\rho_1 g\nu}{4\rho_2\sigma(\nu^2 + G^2/\rho_2^2\sigma^2)}. \tag{3.32}$$

This provides a very convenient expression for predicting the attenuation of long waves that propagate over an almost rigid bed of infinite depth.

The amplitude ratio a_1/a_2 for an almost rigid bed is obtained from the long wave equivalent of equation (3.17) whereby we replace $\sinh mh_1$ by mh_1 and $\cosh mh_1$ by unity. On substituting equation (3.30) into this, we derive an expression for the amplitude ratio:

$$\frac{a_2}{a_1} \approx \frac{2(gh_1)^{\frac{1}{2}}}{\sigma}\left|\frac{\rho_1 gG + i\rho_1\rho_2 g\nu\sigma}{4\rho_2^2\sigma^2(\nu^2 + G^2/\rho_2^2\sigma^2)}\right|, \tag{3.33}$$

where we have neglected higher-order terms.

Given the amplitude of the surface wave, a_1, this expression provides a convenient estimate of the relative displacement at the top of the sea bed. Similarly for the phase shift we find

$$\theta \approx \tan^{-1}(\rho_2 \nu\sigma/G). \tag{3.34}$$

The assumption that underlies this analysis is that long waves, that is $mh_1 \ll 1$, are propagating over an almost rigid bed, that is $|m^2\nu_e/\sigma| \gg 1$.

We now go on to examine the differing circumstances under which either viscous effects dominate or elastic effects dominate.

Viscous effects dominant. When viscous effects dominate elastic effects, then

$$\rho_2 \nu\sigma/G \gg 1,$$

and the decay, from (3.32), becomes

$$\frac{D(gh_1)^{\frac{1}{2}}}{\sigma} \approx \frac{\rho_1(g^3h_1)^{\frac{1}{2}}}{4\rho_2\sigma^2\nu}. \tag{3.35}$$

The decay is inversely proportional to the viscosity and independent of the shear modulus of elasticity. From (3.33), the amplitude ratio becomes

$$\frac{a_2}{a_1} \approx \frac{\rho_1(g^3h_1)^{\frac{1}{2}}}{2\rho_2\sigma^2\nu}. \tag{3.36}$$

It is interesting to note that, even when the elasticity of an almost rigid bed is zero, both (3.35) and (3.36) are valid. This is not so for the reverse case as we shall now see.

Elastic effects dominant. When elastic effects dominate viscous effects, then

$$\rho_2 \nu\sigma/G \ll 1,$$

and the decay, from equation (3.32), becomes

$$\frac{D(gh_1)^{\frac{1}{2}}}{\sigma} \approx \frac{\rho_1\rho_2\nu(g^3h_1)^{\frac{1}{2}}}{4G^2}, \tag{3.37}$$

showing that zero viscosity gives zero decay, which is what we would expect. The amplitude ratio is

$$\frac{a_2}{a_1} \approx \frac{\rho_1(g^3h_1)^{\frac{1}{2}}}{2G\sigma}, \tag{3.38}$$

which is independent of the viscosity. Because the amplitude ratio is inversely proportional to the elasticity G, then with increasing elasticity we have decreasing amplitude ratio and thus the elastic forces are acting to restrain the motion of the bed. In this way we can understand how, with increasing elasticity, the decreasing bed movements result in decreasing attenuation, as shown by equation (3.37).

3.3. *Energy dissipation*

The average rate that energy is dissipated in the non-rigid bed can be evaluated by several methods. Probably the simplest approach is to calculate the mean work done on the lower layer per unit area of the interface. The average rate of energy dissipa-

tion, P, is the average energy transmitted through the interface per unit area and time:

$$P = -\frac{1}{T}\int_0^T \overline{p_1 v_1}\, dt \quad \text{on} \quad y = \eta_2, \tag{3.39}$$

where the overbar denotes the time average and T is the wave period ($2\pi/\sigma$). Using equation (2.11), the linearized form is

$$P = -\frac{1}{T}\int_0^T \overline{(\rho_1 \phi_{1t} - \rho_1 g \eta_2)\,\eta_{2t}}\, dt \quad \text{on} \quad y = 0. \tag{3.40}$$

The interface profile is given by equation (3.3), which on differentiating with respect to time yields

$$\eta_{2t} = a_2 \sigma e^{-Dx} \sin(kx - \sigma t). \tag{3.41}$$

Because the interface η_2 moves in simple harmonic motion whereby η_2 and η_{2t} are always out of phase by $\frac{1}{2}\pi$, the second part of the integrand in (3.40) has zero value:

$$\int_0^T \overline{\eta_2 \eta_{2t}}\, dt = 0. \tag{3.42}$$

To evaluate the first part of the integrand we require to evaluate an expression for ϕ_{1t} on $y = 0$. On differentiating equation (3.14) with respect to time, we obtain

$$\phi_{1t}|_{y=0} = -\frac{B\sigma^2}{2im^2\nu}\left[\frac{gm\cosh mh_1 - \sigma^2 \sinh mh_1}{gm \sinh mh_1 - \sigma^2 \cosh mh_1}\right] \exp[i(mx - \sigma t)]. \tag{3.43}$$

At this stage it is important to recall that we take only the real part of the right-hand side of this equation. Thus, utilizing equation (3.11) and substituting (3.41) and (3.43) into (3.40) and performing the integration, the average rate of energy dissipation is found to be

$$P = -\tfrac{1}{2}\rho_1 g (a_2 e^{-Dx})^2 \sigma \operatorname{Im}\left\{\frac{\sigma^2(gm\cosh mh_1 - \sigma^2 \sinh mh_1)}{gm\,(gm \sinh mh_1 - \sigma^2 \cosh mh_1)}\right\}, \tag{3.44}$$

where m is obtained from the dispersion relation.

To obtain an expression for an energy dissipation which is independent of x we define, following Dalrymple & Liu (1978), the local energy per unit area, E, based on the local wave amplitudes, as

$$E = \tfrac{1}{2}\rho_1 g (a_1 e^{-Dx})^2 + \tfrac{1}{2}(\rho_2 - \rho_1)\, g (a_2 e^{-Dx})^2. \tag{3.45}$$

Then the *relative* energy dissipation per unit time is given by the ratio P/E.

4. Results

4.1. *Discussion of the roots*

In the numerical solution of the dispersion relation equation (3.20), or if the non-rigid bed is of infinite depth (3.26), we evaluate the complex values of m which are the roots that represent a system of progressive waves. (For standing waves, m would be real and σ complex, therefore we would solve for the complex values of σ.) From the roots of the dispersion relation we can determine the basic character of the wave motion such as the rate of attenuation (from the imaginary part of m), the wave-

number (from the real part of m), the ratio of interface to surface wave amplitude and the phase angle between the interface and surface waves. For convenience we introduce the following non-dimensional parameters:

$$\left.\begin{aligned} k^* &= k(gh_1)^{\frac{1}{2}}/\sigma, \quad D^* = D(gh_1)^{\frac{1}{2}}/\sigma, \\ \nu^* &= \nu/(gh_1^3)^{\frac{1}{2}}, \quad G^* = G/\rho_2 g h_1, \\ P^* &= (P/E)\,(h_1/g)^{\frac{1}{2}}, \end{aligned}\right\} \tag{4.1}$$

where P^* is a non-dimensional form of the relative energy dissipation rate. Throughout the presentation of the results we take the surface tension to be negligible and we take the lower layer to be of infinite depth. In figures 2 to 6 we plot results for a radian frequency $\sigma^* = 0{\cdot}5$ and density ratio $\rho^* = 0{\cdot}5$. For a water depth of 10 metres, say, then this radian frequency corresponds to a wave period of around 12 seconds. The density ratio is based on a lower layer *in situ* density of $2{\cdot}0$ g cm^{-3} which corresponds to a saturated sand with dry density $2{\cdot}6$ g cm^{-3} and void ratio $0{\cdot}6$.

To investigate physically reasonable solutions to the dispersion relation (3.26), we will first discuss the special case where the bed elasticity is negligible (i.e. $G \to 0$). If in addition viscous effects are neglected then equation (3.26) reduces to the classical dispersion relation for two inviscid layers of fluid of different density where two types of wave motion are possible (Lamb 1932). The first type of wave is identical to the ordinary surface wave which has a wavenumber $m = \sigma^2/g$; it is called an 'external' wave, because the upper surface has the larger amplitude, and the surface and interface are in phase. The second type of wave, which has the larger amplitude at the interface, is called an 'internal' wave and the surface and interface are of opposite phase.

Returning to the dispersion relation (3.26) but with zero elasticity, along the lines of § 3.2 we can show that for small viscosity, i.e. $\nu^* \ll 1$, there are two possible solutions and that they are related to the external and internal waves of the inviscid problem. For example the small-viscosity solution with the external wavenumber is found to be

$$m \approx \frac{\sigma^2}{g} + \frac{4i\nu\sigma^5}{g^3}, \tag{4.2}$$

yielding a decay

$$D \approx \frac{4\nu\sigma^5}{g^3}. \tag{4.3}$$

The small-viscosity solution that is related to the internal wavenumber yields a decay which though proportional to the viscosity is of a greater order of magnitude for physically realistic parameters. Because the decay (4.3) associated with external wavenumber $m = \sigma^2/g$ is smaller, it is this solution which is of physical importance in that it describes waves that dissipate more slowly.

An analysis for large viscosity $\nu^* \gg 1$, as has been done in § 3.2 but with $\nu_e \to \nu$, yields the complex wavenumber

$$m \approx \frac{\sigma}{(gh)^{\frac{1}{2}}} + \frac{i\rho_1 g}{4\rho_2 \sigma \nu}, \tag{4.4}$$

the real part being the long-wave rigid-bed wavenumber and the imaginary part being the decay

$$D \approx \frac{\rho_1 g}{4\rho_2 \sigma \nu}. \tag{4.5}$$

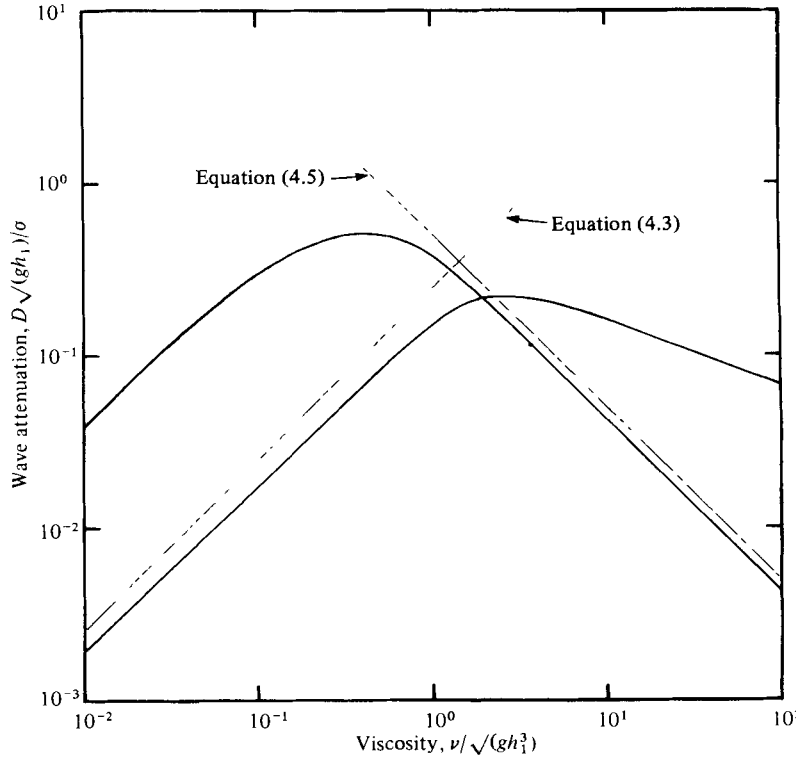

FIGURE 2. Viscous bed attenuation D^* for different modes of oscillation with elasticity $G^* = 0$, $h_2 = \infty$, $\sigma^* = 0{\cdot}5$ and $\rho^* = 0{\cdot}5$.

For this large-viscosity solution the decay is closely related to the 'creeping' mode which, with the 'viscous' mode, is a solution to the problem of wave motion at the surface of a very viscous semi-infinite medium [Wehausen & Laitone 1960, equation (25.24)]. The 'creeping' mode has a decay inversely proportional to the viscosity while the 'viscous' mode has a more rapid decay which is inversely proportional to $\nu^{\frac{1}{2}}$. Both these modes represent aperiodic motions; i.e. the fluid slowly returns to its equilibrium state. When water waves are propagating over a viscous bed, however, a considerable proportion of the total energy is in the upper inviscid layer and therefore the resulting wave motion will be periodic as given by (4.4).

To illustrate this discussion of the roots we plot, in figure 2, with viscosity ν^* as abscissa and decay D^* as ordinate, solutions to the dispersion relation (3.26) with $G^* = 0$ that yield positive decay. We reject solutions with negative decay because a disturbance that grows in amplitude with distance is physically unacceptable. For the small-viscosity domain the two possible solutions are related to the 'external' and 'internal' wave motions discussed above; equation (4.3), which is plotted on figure 2, gives a good approximation to the slower decay. For the large-viscosity domain there are again two possible solutions which this time are related to the 'creeping' and 'viscous' modes discussed above, i.e. proportional to ν^{*-1} as given approximately by equation (4.5) and to $\nu^{*-\frac{1}{2}}$ respectively. Because we are primarily interested in the root that yields the longest-living wave, it is clear from figure 2 that

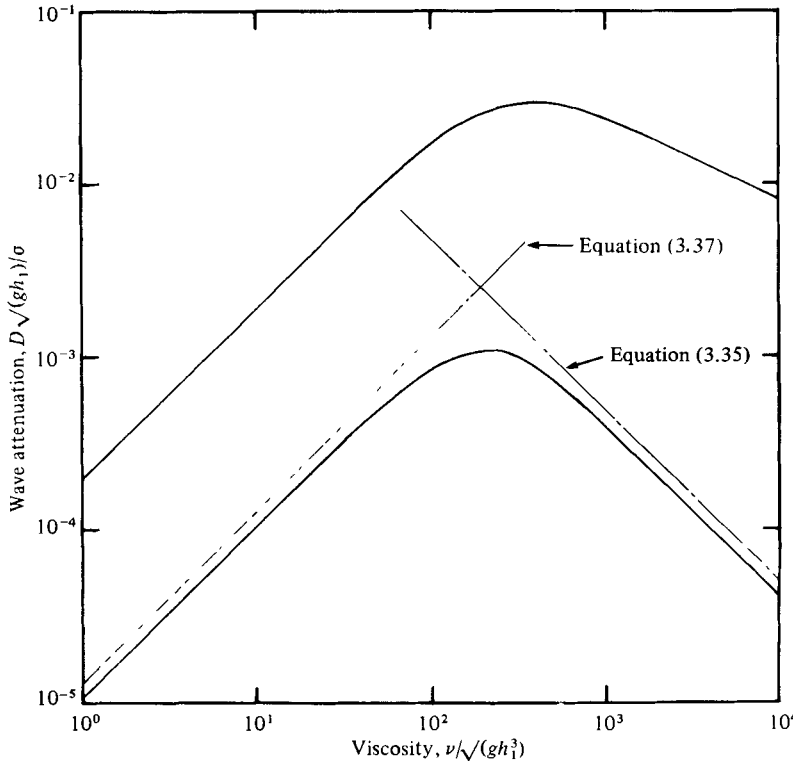

FIGURE 3. Viscoelastic bed attenuation D^* for different modes of oscillation with elasticity $G^* = 100$, $h_2 = \infty$, $\sigma^* = 0{\cdot}5$ and $\rho^* = 0{\cdot}5$.

there is an apparent discontinuity at a viscosity of around $\nu^* = 2{\cdot}0$ between the appropriate root for the small- and for the large-viscosity domains.

Where waves propagate over a bed that is viscoelastic, the types of solutions are similar to those discussed above for a purely viscous bed. For example we take the case of $G^* = 100$ and plot the solutions to the dispersion relation equation (3.26) in figure 3. As for the case of a viscous bed, after rejecting roots that lead to a negative decay there are two possible solutions. In the region where elastic effects dominate, i.e. $\rho_2\sigma\nu/G \ll 1$, the two modes both yield a decay proportional to ν^*, the slower decay rate being given approximately by equation (3.37). Where viscous effects dominate, i.e. $\rho_2\sigma\nu/G \gg 1$, the two modes are proportional to ν^{*-1} and $\nu^{*-\frac{1}{2}}$, the slower decay being represented approximately by equation (3.35).

In the next section, numerical results will be presented for a physically realistic range of the elasticity parameter G^*. For clarity only results for the root that yields the slower decay will be plotted.

4.2. *Numerical results for viscoelastic bed*

In figures 4 to 6 we plot results for waves propagating over a non-rigid bed within which there is both a viscous and an elastic response. For a water depth of 10 metres, say, the viscosity values on the abscissa range from 10^5 cm^{2}s^{-1} to 10^{13} cm^2 s^{-1} and

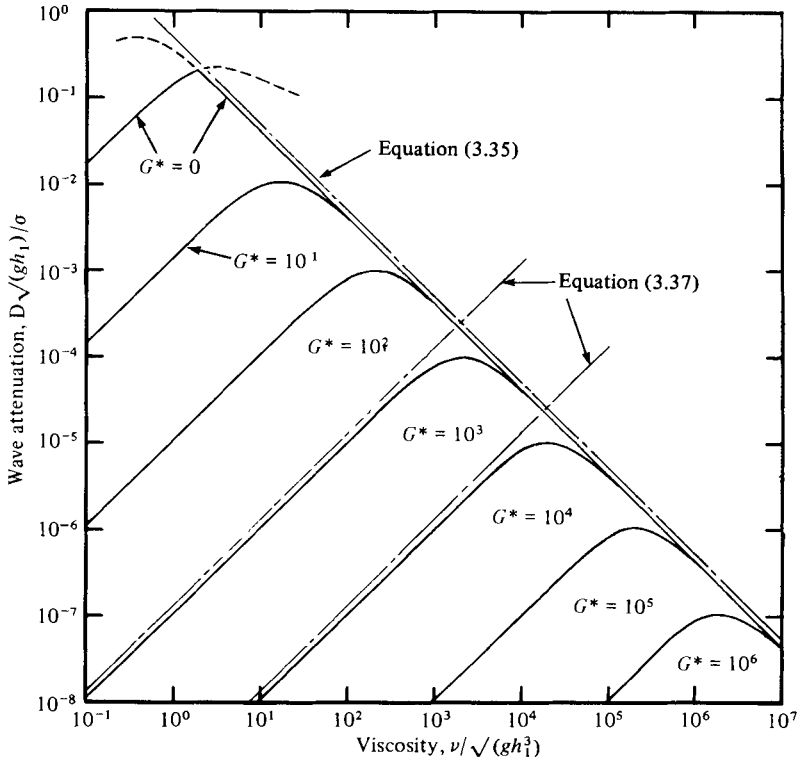

FIGURE 4. Wave attenuation D^* plotted against viscosity ν^* for varying elasticity G^* with $h_2 = \infty$, $\sigma^* = 0{\cdot}5$ and $\rho^* = 0{\cdot}5$. The dashed extensions represent the root yielding more rapid attenuation.

for the elasticity parameter, values range from 2×10^7 dyne cm^{-2} to 2×10^{12} dyne cm^{-2}. For larger values of either viscosity or elasticity, it will be shown that the bed has negligible effect on the waves.

In figure 4 the wave attenuation D^* is again plotted as ordinate with elasticity as parameter for the family of curves. With increasing values of the elasticity G^*, the peaks in the attenuation are of a successively lower magnitude. The straight line to the right of the peaks is given by equation (3.35) and the lines to the left of the peaks are given by equation (3.37). When neither the viscous nor the elastic effects dominate (and from § 3.2 we know that the balance between the two effects occurs when the parameter $\rho_2 \sigma \nu / G$ is of order unity) there is a local peak in the wave attenuation.

In figure 5 we plot as ordinate the ratio of the interface to the surface amplitude, a_2/a_1. For negligible elasticity, i.e. when $G^* \to 0$, there is a discontinuity in the amplitude ratio which corresponds to the intersection point between the small- and large-viscosity solutions discussed above. For the viscoelastic cases, with increasing elasticity there is a corresponding decrease in the maximum amplitude ratio showing that the elastic forces are restraining the motion of the bed. We can divide the figure into two zones; firstly where the viscous effects dominate, i.e. $\rho_2 \sigma \nu / G \gg 1$, the amplitude ratio is given approximately by equation (3.36) as plotted, secondly where elastic effects dominate, i.e. $\rho_2 \sigma \nu / G \ll 1$, the amplitude ratio tends to the horizontal asymptotes given by equation (3.38).

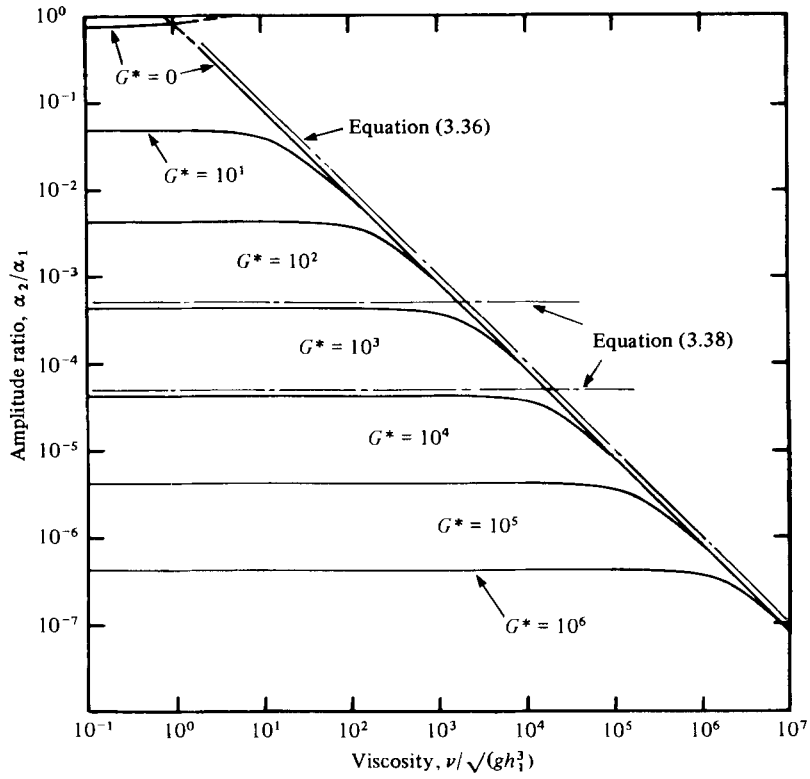

FIGURE 5. Ratio of interface amplitude to surface wave amplitude with $h_2 = \infty$, $\sigma^* = 0{\cdot}5$ and $\rho^* = 0{\cdot}5$. The dashed extensions represent the root yielding more rapid attenuation.

In figure 6 we plot the phase angle θ between the surface profile and the interface profile. In the purely viscous case, i.e. when $G^* \to 0$, for the small-viscosity solution $0 < \theta < \frac{1}{2}\pi$, and for the large-viscosity solution $\pi < \theta < \frac{1}{2}\pi$, with the discontinuity at the intersection point of the two solutions. For the viscoelastic cases when elastic effects dominate $\theta \approx \pi$, and when viscous effects dominate $\theta \approx \frac{1}{2}\pi$.

It is appropriate at this point to comment on the numerical results of Gade (1959). He limits his numerical discussion to the case where elastic effects dominate; for example his results for wave attenuation are represented only by the lower left half of figure 4. He finds that the surface and interface profile are out of phase by π and for decreasing values of the elasticity parameter there is increasing decay and increasing amplitude ratio. In the present theory however it has been shown that these occur only where elastic effects dominate. Gade's paper does not show that viscous effects can dominate nor that the peak in the decay occurs when the viscous and elastic effects are balanced.

4.3. *Comparison of wave dissipation mechanisms*

In coastal waters, the dissipation of wave energy is usually the result of some form of bottom interaction. For most mechanisms of energy dissipation, such as those due to bottom friction, the formation of a laminar boundary layer or percolation in a permeable bed, it is assumed that the bed is rigid. In this section we compare the energy dissipation rates for these rigid-bed mechanisms with the rates for the non-rigid-bed mechanism of the present theory.

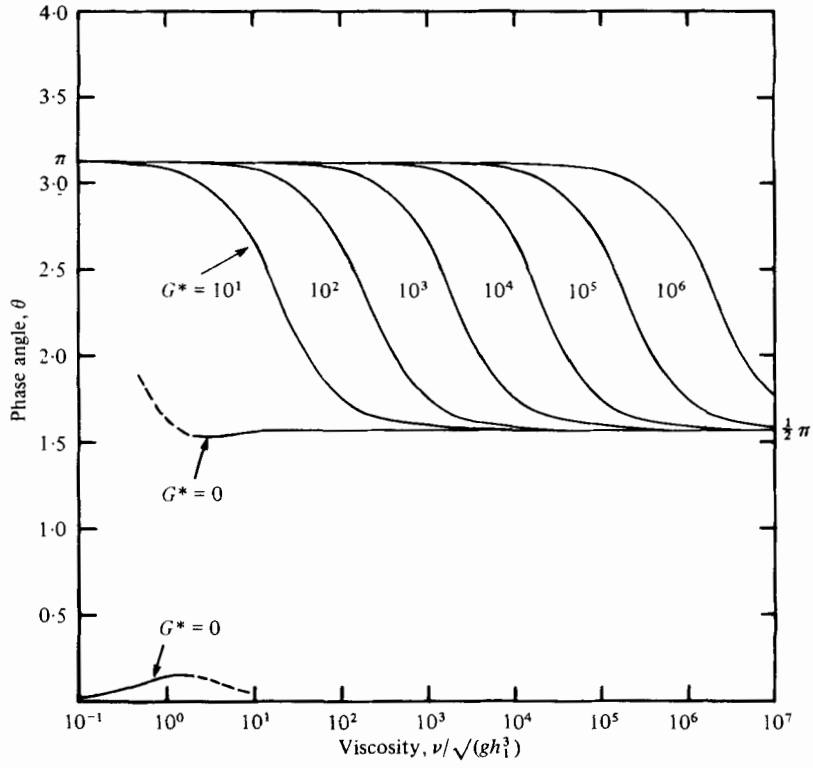

FIGURE 6. Phase angle between surface and interface profile with $h_2 = \infty$, $\sigma^* = 0{\cdot}5$ and $\rho^* = 0{\cdot}5$. The dashed extensions represent the root yielding more rapid attenuation.

In figure 7 we plot, with radian frequency σ^* as abscissa, wave energy dissipation rates P^* for the following.

(*a*) A viscous bed with elasticity $G^* = 0$ and viscosity $\nu^* = 10^{-1}$ and density $\rho^* = 0{\cdot}8$ corresponding to soft mud. In figure 7 we see that this case gives the most rapid wave damping with the energy dissipation $P^* \approx 0{\cdot}05$.

(*b*) A viscoelastic bed with the elasticity $G^* = 10$, viscosity $\nu^* = 10$ and $\rho^* = 0{\cdot}5$. For this case the peak in the energy dissipation is $P^* \approx 0{\cdot}01$.

(*c*) An almost rigid viscoelastic bed with an elasticity $G^* = 10^2$, $\nu^* = 10^2$ and $\rho^* = 0{\cdot}5$. Here the peak in the energy dissipation occurs at $P^* \approx 0{\cdot}001$.

(*d*) Bottom friction dissipation, P_f, as given by Putnam & Johnson (1949), is

$$\frac{P_f}{\frac{1}{2}\rho_1 g a_1^2} = \frac{4 f a_1 \sigma^3}{3\pi g (\sinh k h_1)^3}, \tag{4.6}$$

where f is the friction coefficient, which we take to be 10^{-2}, as used by most workers, and we take the ratio $a_1/h_1 = 0{\cdot}15$. In figure 7, we see that the dimensionless dissipation $P_f^* \approx 0{\cdot}0006$ for the lower frequencies, but gradually decreasing for increasing radian frequency. Clearly the rate of energy dissipation is very dependent on the choice of f and a_1/h_1.

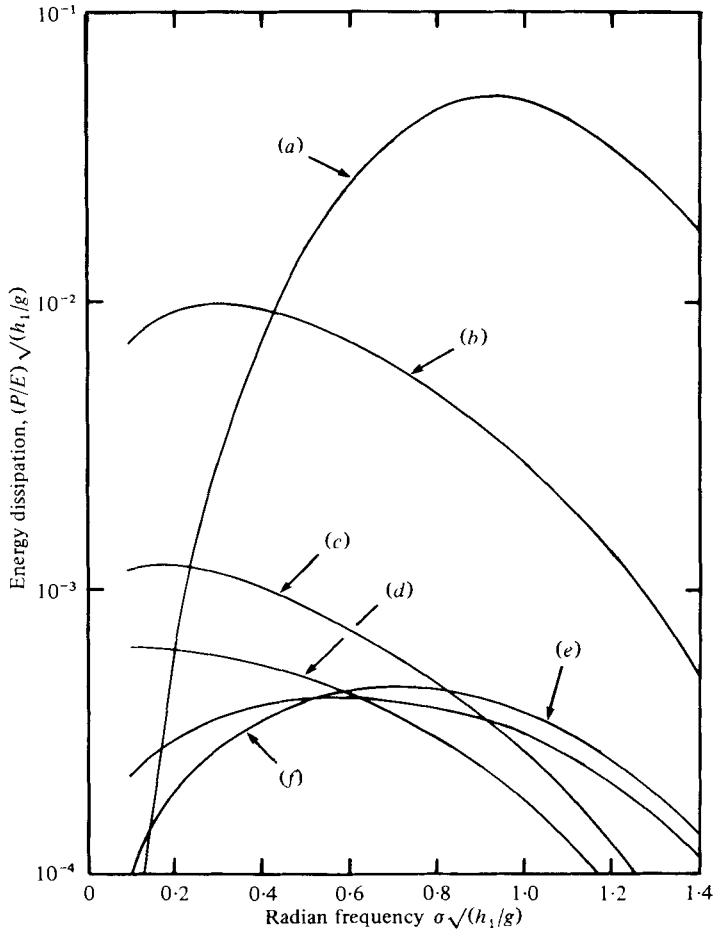

FIGURE 7. Comparison of wave energy dissipation mechanisms for the following: (*a*) viscous bed $G^* = 0$, $\nu^* = 10^{-1}$, $h_2 = \infty$, $\rho^* = 0{\cdot}8$; (*b*) viscoelastic bed $G^* = 10$, $\nu^* = 10$, $h_2 = \infty$, $\rho^* = 0{\cdot}5$; (*c*) viscoelastic bed $G^* = 100$, $\nu^* = 100$, $h_2 = \infty$, $\rho^* = 0{\cdot}5$; (*d*) bottom friction with friction coefficient $f = 10^{-2}$ and the ratio $a_1/h_1 = 0{\cdot}15$; (*e*) laminar boundary layer; and (*f*) permeable bed with hydraulic conductivity $\kappa = 0{\cdot}01$ m s^{-1}.

(*e*) Laminar boundary layer dissipation, P_b, as given by Ippen (1966), is

$$\frac{P_b}{\frac{1}{2}\rho_1 g a_1^2} = \frac{gk^2\nu^{\frac{1}{2}}}{(2\sigma^3)^{\frac{1}{2}}\cosh^2 kh_1}, \tag{4.7}$$

where ν is the viscosity of water. The peak dissipation is around $P_b^* \approx 0{\cdot}0005$.

(*f*) Permeable bed dissipation, P_p, as given by Reid & Kajiura (1957), assuming the bed is of infinite depth, is

$$\frac{P_p}{\frac{1}{2}\rho_1 g a_1} = \frac{gk\kappa}{\cosh^2 kh_1}, \tag{4.8}$$

where κ is the hydraulic conductivity (coefficient of permeability), which for an average coarse sand is 0·01 m s^{-1}. For this mechanism of dissipation we see that the peak is at $P_p^* \approx 0{\cdot}0005$.

Comparing the magnitude of the energy dissipation by the various mechanisms, we see from figure 7 that the viscous bed, curve (*a*), gives a peak energy dissipation that is considerably greater than the viscoelastic bed of curve (*b*), which is more than one order of magnitude greater than either the viscoelastic bed of curve (*c*) or the other mechanisms of energy dissipation of curves (*d*), (*e*) and (*f*). The rate of energy dissipation for a non-rigid bed is very dependent on the values of viscosity and elasticity within the bed. In the absence of adequate *in situ* measurements, in figure 7 we have used viscosity and elasticity values for which the rates of energy dissipation are of the same order of magnitude or greater than the energy dissipation rates when the bed is rigid.

5. Discussion

5.1. *Waves over an almost rigid bed*

This investigation of wave attenuation may provide a clue to the explanation of swell decay rates as observed in the North Sea by Hasselmann *et al.* (1973). They found that the theory of wave attenuation due to bottom friction gave decay rates of the correct order of magnitude but that the theory was contradicted because there was no modification of the decay rates by the strong tidal currents. They concluded that: 'We have not been able to identify clearly the mechanism of swell attenuation' (Hasselmann *et al.* p. 89). Because the strongest decay rate was observed close to the shore, they suspect that some form of bottom interaction is important. As we have shown above, the mechanism of attenuation due to a non-rigid bed (which yields decay rates that are independent of the tidal currents) can give, depending on the sea-bed elasticity and viscosity parameters, decay rates that are the same order of magnitude as those predicted by bottom friction and also as those observed in the North Sea.

To illustrate this, we take a radian frequency of $\sigma^* = 0{\cdot}5$, a viscosity of $\nu^* = 10^2$ and an elasticity of $G^* = 10^2$ because these parameters are known to yield wave attenuation rates of the same order of magnitude as bottom friction and percolation, see § 4.3. For a water depth of 10 metres, say, the radian frequency corresponds to a swell wave period of around 12 seconds, the viscosity parameter corresponds to a kinematic viscosity of 10^8 cm^2 s^{-1} and with $\rho_2 = 2{\cdot}0$ g cm^{-3} the elasticity parameter corresponds to a shear modulus of elasticity of approximately $2{\cdot}0 \times 10^8$ dynes cm^{-2}.

From the numerical calculations, we find that the wavenumber $k^* = 1{\cdot}045$ (i.e. close to the rigid-bed long-wave wavenumber of unity) which corresponds to a wavelength of approximately 120 metres. The decay, from figure 4, is $D^* = 0{\cdot}00084$, which can be recalculated to give the dimensional decay $D = 0{\cdot}005/L$. By our definition a wave decays with distance as $\exp(-Dx)$ and so for this case the wave travels a distance of 200 wavelengths before the wave amplitude is reduced to $e^{-1} = 0{\cdot}37$ of the original amplitude.

The ratio of interface to surface wave amplitude is, from figure 5, $a_2/a_1 = 0{\cdot}0037$. Thus a surface wave amplitude of 1·5 metres, say, results in an amplitude at the top of the bed of approximately 0·005 m. This gives a total deflexion (i.e. wave height) of around 1 cm, a figure not inconsistent with the sea-bed deflexions in the North Sea of up to 5 cm as reported by Bjerrum (1973), where possibly the wave heights were much larger.

5.2. *Waves over a soft muddy bed*

Extraordinarily rapid wave damping has been observed at the mud flats off the south-west coast of India. The mud flats are characterized by an *active* phase during the stormy monsoon season when there is strong wave attenuation at the seaward edge and by a *passive* phase during the calmer non-monsoon months when the mud flats appear to have little effect on the waves. During the active phase each mud flat, or mud bank as they are called, is clearly marked by a semi-circular area of calm water stretching 5 to 7 km alongshore and extending 3 to 4 km offshore, outside of which there are rough monsoon seas. At the outer edge of the mud flat area, at a water depth of around 10 to 12 metres, there is a peripheral zone within which the waves are almost completely attenuated over a distance of 4 to 8 wavelengths (MacPherson & Kurup 1979).

Observations of rapid decay rates have been made at other localities. Gade (1958) mentions a place called the Mud Hole on the Louisiana coast where the viscous bed has a pronounced calming effect on the sea in rough weather. On the west coast of Malaysia, Silvester (1974, and personal communication) has observed 'waves of around 4 seconds arriving in mud flats and in a matter of a few wavelengths are completely attenuated' (Silvester 1974, p. 196).

The first theoretical analysis of such phenomena was undertaken by Gade (1958). Dalrymple & Liu (1978) have recently analysed this problem, namely of predicting the attenuation of waves propagating over a viscous bed. They use small-amplitude wave theory for studying the coupled interaction between the two layers, but where they differ from the present analysis is in their inclusion of viscous effects in the upper layer. This approach may be more complete mathematically, but it does not lead to the relatively simpler dispersion relation in the form of a single equation (3.20).

Returning to the present theory we now discuss a numerical example of severe wave attenuation by taking a radian frequency $\sigma^* = 0{\cdot}5$, viscosity $\nu^* = 1{\cdot}0$ and elasticity $G^* = 0$. For a water depth of 10 m, these parameters give a wave period of roughly 12 seconds, which is the dominant swell wave period during the monsoon months at the Indian mud flats, and a kinematic viscosity of 10^6 cm^2 s^{-1} (larger than might be expected from the exploratory experimental investigations of MacPherson & Kurup 1979). We take the lower layer to be of infinite depth and we take the lower-layer density to be 1·25 g cm^{-3}, i.e. a density ratio $\rho^* = 0{\cdot}8$, because measurements indicate that for soft muddy sea beds the *in situ* density can be as low as this (MacPherson & Kurup 1978).

From the numerical calculations we find that the wavenumber is $k^* = 0{\cdot}462$, which corresponds to a wavelength of 272 metres. The wavenumber is close to the aforementioned 'external' wavenumber of $k = \sigma^2/g$. The decay is found from figure 7 to be $D^* = 0{\cdot}152$, which can be rewritten as $D = 2{\cdot}1/L$. Therefore the wave has to travel only 1·1 wavelengths before its amplitude is reduced to 10 % of its original amplitude!

If we had taken the viscosity as $\nu^* = 3{\cdot}0$ (instead of $\nu^* = 1{\cdot}0$ as above), with all other parameters the same, we would get a wavenumber $k^* = 1{\cdot}05$ which is very close to the rigid-bed wavenumber obtained from $\sigma^2 = kg \tanh kh_1$. The decay is $D^* = 0{\cdot}14$ or $D = 0{\cdot}827/L$, where the wavelength L is 120 m. Thus the wave travels 2·8 wavelengths before its amplitude is reduced to 10 % of its original amplitude. Comparing this result (where $\nu^* = 3{\cdot}0$) with the first result above (where $\nu^* = 1{\cdot}0$)

we have almost the same rate of attenuation with horizontal distance because in either case the wave has to travel around 300 m for the amplitude to decay to 10% of its original amplitude.

For either case of this albeit extreme example, the predicted wave attenuation is more rapid than observed rates of wave attenuation at the mud flats off the south west coast of India where waves are said to almost completely 'disappear' over a distance of 4 to 8 wavelengths.

5.3. *Concluding remarks*

For water waves propagating over a viscoelastic bed, a dispersion relation in the form of a single equation has been derived. Physically reasonable solutions are discussed and numerical results for wave attenuation and the relationship between the interface and surface wave profiles are presented. The rate of attenuation is largely dependent on the magnitude of the viscosity and elasticity parameters in the bed. When the magnitudes of these parameters are within an intermediate range, the bed is almost rigid in response to wave action and yet significant rates of wave attenuation can be predicted. This mechanism may be a contributing factor in the attenuation of waves over continental shelves and in coastal waters. For the limiting case of an inelastic fluid bed, there are no elastic forces to restore the bed to its undisturbed position, and as a result large oscillations in the bed and extremely rapid rates of attenuation can occur.

I wish to thank J. D. Fenton for his interest and encouragement in this work.

REFERENCES

BJERRUM, L. 1973 Geotechnical problems involved in foundations of structures in the North Sea. *Geotech.* **23**, 319–358.

BROMWICH, B. A. 1898 On the influence of gravity on elastic waves. *Proc. Lond. Math. Soc.* **30**, 98–120.

DALRYMPLE, R. A. & LIU, P. L. 1978 Waves over soft muds: a two layer model. *J. Phys. Oceanog.* **8**, 1121–1131.

GADE, H. G. 1958 Effects of a non-rigid, impermeable bottom on plane surface waves in shallow water. *J. Mar. Res.* **16**, 61–82.

GADE, H. G. 1959 Notes on the effects of elasticity of bottom sediments to the energy dissipation of surface waves in shallow water. *Arch. Math. Natur.* **55**, 1–12.

HASSELMANN, K., BARNETT, T. P., BOUWS, E., CARLSON, H., CARTWRIGHT, D. E., ENKE, K., EWING, J. A., GIENAPP, H., HASSELMANN, D. E., KRUSEMAN, P., MEERBURG, A., MULLER, P., OLBERS, D. J., RICHTER, K., SELL, W. & WALDEN, H. 1973 Measurements of wind-wave growth and swell decay during the Joint North Sea Wave Project. *Deutsch. Hydrograph. Inst.* A **80**, 1–95.

IPPEN, A. T. 1966 *Estuary and Coastline Hydrodynamics.* McGraw-Hill.

KOLSKY, H. 1963 *Stress Waves in Solids.* Dover.

LAMB, H. 1932 *Hydrodynamics*, 6th edn. Cambridge University Press.

MACPHERSON, H. & KURUP, P. G. 1979 Wave damping at the Kerala mudbanks, south-west India. Submitted to *Indian Mar. Sci.*

MALLARD, W. W. & DALRYMPLE, R. A. 1977 Water waves propagating over a deformable bottom. *Proc. Offshore Tech. Conf.*, OTC 2895, pp. 141–146.

PUTNAM, J. A. & JOHNSON, J. W. 1949 The dissipation of wave energy by bottom friction. *Trans. Am. Geophys. Union* **30**, 67–74.

REID, R. O. & KAJIURA, K. 1957 On the damping of gravity waves over a permeable sea bed. *Trans. Am. Geophys. Union* **38**, 662–666.

SILVESTER, R. 1974 *Coastal Engineering*. Elsevier.

TCHEN, C. 1956 Interfacial waves in viscoelastic media. *J. App. Phys.* **27**, 431–434.

WEHAUSEN, J. V. & LAITONE, E. V. 1960 Surface waves. In *Handbuch der Physik*, vol. 9, 3. Springer.